Synthetic polymer composite membrane for the desalination of saline water

M.A. Ashraf[a,*], M.J. Maah[a], A.K. Qureshi[a], M. Gharibreza[b], I. Yusoff[b]

[a]*Department of Chemistry, University of Malaya, Kuala Lumpur 50603, Malaysia*
Tel. +60 172770972; Fax: +60 379675149; email: chemaqeel@gmail.com
[b]*Department of Geology, University of Malaya, Kuala Lumpur 50603, Malaysia*

ABSTRACT

Development of desalination technologies has been identified as vital to fulfilling future water demand. In this research, composite membrane with polyvinyl alcohol (PVA) as separating layer material while cellulose acetate (CA) and polyethylene glycol (PEG) as supporting layer material were used. In the present research work, the synthesis and characterization of a multilayer PVA/CA/PEG membrane was attempted where membrane performance and applicability were investigated for reverse osmosis desalination of different feed concentrations of groundwater, brackish, highly saline, and also extremely saline water (seawater). Values of both salt rejection and water flux were assessed as a measure of membrane efficiency. In addition to suitable application of the prepared synthetic membranes, the antimicrobial sustainability was also evaluated where prospective function against gram-positive and gram-negative bacteria was depicted. It can be concluded by this work that multilayer PVA/CA/PEG membrane performed excellently for the desalination of groundwater, brackish, highly saline, and also extremely saline water. The flux reduction was reduced significantly when PEG was incorporated in the composite membrane. The importance of structural differences for antimicrobial activity of the prepared membranes has been studied with the use of gram-negative and gram-positive bacteria. Antimicrobial efficiency improves with the use of PEG and membranes with smaller pore sizes.

Keywords: Reverse osmosis; Polyvinyl alcohol; Polyethylene glycol; Cellulose acetate; Salt rejection; Water flux; Feed concentration; Antimicrobial activity

1. Introduction

Water is essential for the survival of all forms of life on earth. On an average, a human being consumes about 2 l of water every day [1]. Water accounts for about 70% of the weight of a human body [2]. Today, access to clean water is becoming a difficult task in many regions of the world. According to the World Health Organization, 1.2 billion people lack access to sufficient amounts of clean fresh water and 2.6 billion lack adequate sanitation [3]. Poor sanitation combined with unhealthy water quality accounts for the largest single cause for disease and death in the world. About 75% part of the earth is covered with water and out of which 97% is saltier and only 3% is available for drinking, agriculture, domestic, and industrial consumption [4]. Fresh water is about 2.8% of the total

*Corresponding author.

water in the world, whereas among fresh water, only 0.6% is available for use while the rest is locked up in oceans as salt water, polar ice caps, glaciers, and underground reservoirs [5].

The need for fresh clean water is growing rapidly due to the world population growth that imposes larger demands of water supply for domestic use, agriculture, and industry. Another reason is deterioration of fresh water supplies: aquifers, the largest fresh water resource, are being contaminated constantly by industrial and agricultural activities, as well as by intrusions of seawater or saline water due to overuse. Rivers and lakes (surface water resources) are also in threat. Hence, there is a strong need to increase fresh water availability either by recycling waste water or by production of fresh water from seawater [6]. The need to increase fresh water supply and more extensive water treatment drove the advancement of new water technologies and the maturity of existing ones, in all fields of water: desalination and ion removal by reverse osmosis (RO), disinfection techniques by catalysts and by biological treatment, decontamination, new filtration techniques, and monitoring of water quality.

Desalination is a general term for methods to remove salt from salty water to produce fresh water. Notably, the definition of fresh water depends on the country. For example, the US Environmental Protection Agency has nonenforceable standards of 250 mg/L chloride and 500 mg/L total dissolved salts (TDS) for fresh water [7]. The World Health Organization (WHO) and the Gulf Drinking Water standards recommended a drinking water standard of 1000 mg/L TDS [8]. In comparison to the government standards, most desalination facilities are designed to achieve a TDS of 500 mg/L or less [9]. When the desalinated water is used for other purposes, e.g. crop irrigation, the TDS concentration may be higher. The feedwater salinity for desalination facilities ranges from 1,000 mg/L to 60,000 mg/L. Most of the seawater resources contain 30,000 to 45,000 mg/L TDS, while the brackish water within a range of 1,000–10,000 mg/L is treated by reverse osmosis (RO) [10].

As mentioned above, desalination occurs by two methods, i.e. by thermal process (multistage flash) or by membrane (RO). Osmosis is a natural phenomenon in which a solvent (usually water) passes through a semipermeable barrier from the side with lower solute concentration to the higher solute concentration side [11] as shown in Fig. 1(a); water flow continues until chemical potential equilibrium of the solvent is established. At equilibrium, the pressure difference between the two sides of the membrane is equal to the osmotic pressure of the solution. To reverse the flow of water (solvent), a pressure difference greater than the osmo-
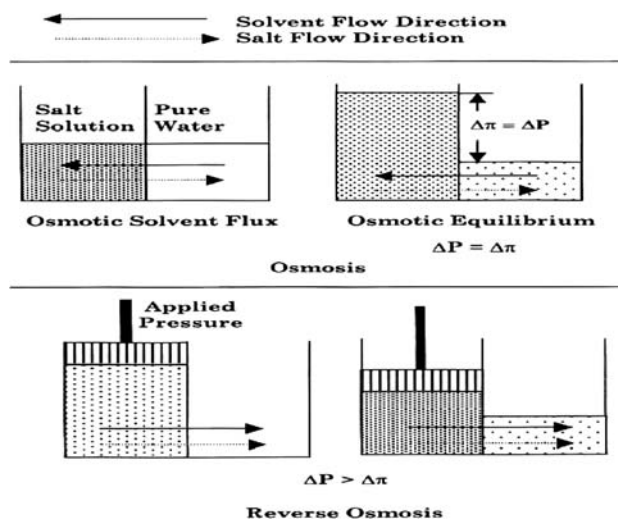

Fig. 1. Schematic of osmosis and RO phenomena.

tic pressure difference is applied as shown in Fig. 1(b); as a result, separation of water from the solution occurs as pure water flows from the high concentration side to the low concentration side. This phenomenon is termed RO [12]. RO is based on two variables: high flux of water and high salt rejection. It operates at pressures of 1–10 MPa. It is one of the most efficient systems based on the energy spent per m³ of fresh water produced from seawater. Reverse osmosis rejects nearly all dissolved compounds. General schematic of RO is illustrated as: Water abstraction → pre-treatment → membrane separation unit → post-treatment → distribution [13].

The concepts of "osmosis" and "RO" have been known for many years. In fact, studies on osmosis were carried out as early as 1748 by the French scientist Nollet, and many researchers investigated these phenomena over the next two centuries [14,15]. However, the use of RO as a feasible separation process is a relatively young technology. For RO, semipermeable membranes are used to separate solutes present in the solution. RO membranes fall into two categories: asymmetric membranes and thin-film composite (TFC) membranes. In fact, only in the late 1950s did the work of Reid show that cellulose acetate (CA) RO membranes were capable of separating salt from water, even though the water fluxes obtained were too small to be practical [16–19]. Then, in the early 1960s, Loeb and Sourirajan developed a method for making asymmetric CA membranes with relatively high water fluxes and separations, thus making RO separations both possible and practical [20–22]. TFC membranes are composed of a thin polymer layer on a porous support (polysulfone) and a support backing

(polyester cloth). In TFC, cross-linked aromatic polyamides are the most commonly used polymer. These polymers are more beneficial than CA. It displays stronger resistance to bacterial degradation and does not hydrolyze. It is stable under a wider pH of 4–11 compared to a pH of 4–7. The water in polyamide moves by "jumps" between weakly localized sites. Water oscillates around localized sites until events, such as thermal fluctuations, enable another jump. Salt diffusion in the polymer depends on both Na^+ and Cl^- to satisfy electroneutrality.

Despite the potential to address key issues surrounding global water and energy demands, osmotically driven membrane processes have yet to progress significantly beyond conceptualization. The major obstacle to advancing this technology is the lack of an adequate membrane. A membrane designed for an osmotically driven process should reject dissolved solutes, produce high permeate water fluxes, be compatible with the selected draw solution, and the mechanical stresses generated by the operating conditions. Existing commercial membranes lack one or more of the abovementioned characteristics, inhibiting their use in osmotically driven membrane processes. The purpose of this research is to develop a TFC membrane that can tolerate wide pH ranges, higher temperatures, and harsh chemical environments, and that have highly improved water flux and solute separation characteristics during various RO applications such as seawater and brackish water desalination, wastewater treatment, production of ultrapure water, water softening, and food processing.

2. Materials and methods

2.1. Chemicals and reagents

Polyvinyl alcohol (PVA) of a molecular weight 133,000 g/mol, CA of 39.6% acetyl content average (Mw = 50,000), polyethylene glycol (MW avg. 400), maleic acid, and methanol were provided from Merck. Deionized water (DI) was obtained from Maxima Ultra Pure Water, Elga-Prima Corp, UK with a resistivity of 18 cm. solvents and inorganic salts were of reagent grade and used directly without further purification.

2.2. Preparation of microporous poly (vinyl alcohol) support membrane

Poly (vinyl alcohol) casting solution was prepared by dissolving 5 wt.% (PVA) in water at 90℃ with constant stirring until homogenous solution was obtained. About 0.001 wt.% of the maleic acid as cross-linking agent was then added. The polymer solution was then allowed to cast over a glass plate and subsequently placed in an oven at 50℃ overnight and finally washed with deionized water before further treatment. The effect of maleic acid concentration on the support membrane (PVA) durability was followed by varying its concentration from 0.001 to 0.6 wt.% at reaction periods of 10–90 min. Fig. 2 illustrates the reaction mechanism between PVA and fumaric acid as an analog to that of PVA and maleic acid.

2.3. Fabrication of composite membranes (dip coating method)

CA was dissolved in methanol at different concentrations of 5, 25, 40, and 60 wt.%. The solution was deposited coherently onto the top surfaces of different samples of the PVA support membrane. PEG was then added to the casting mixture to increase the porosity of the cast membrane while maintaining a high polymer content (15–20%) and, therefore, sufficiently high viscosity of the casting mixture [20,21]. Graphical representation of the final polymer composite membrane structure after the casting process is shown in Fig. 3.

The composite membrane environmental location is schematically represented in Fig. 4.

2.4. Membrane characterization and functional features

Structural and functional studies of the PVA/CA grafted RO membranes were conducted and evaluated through the following analytical, functional, and performance techniques.

2.4.1. Surface and topographical studies of membrane

The surface morphologies of the hydrogels as well as the surface of the membranes were investigated by scanning electron microscopy (SEM) images using Quanta 200 FEL, Phillips, Czechoslovakia. The poly-
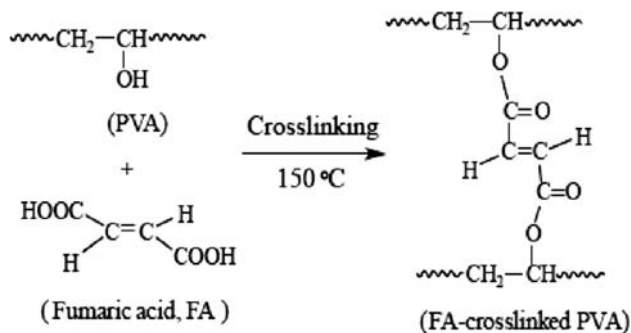

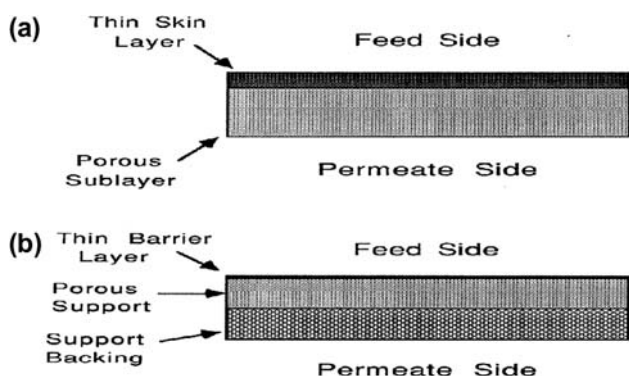Fig. 2. Schematic cross-linking mechanism of PVA with fumaric acid.

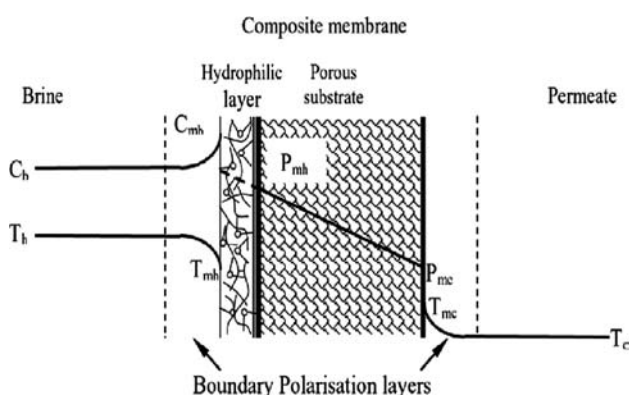Fig. 3. Schematic of (a) asymmetric membrane and (b) TFC membrane.

Fig. 4. Schematic representation of PVA/CA composite membrane environment.

mer films were gold coated before the study. Photographs were taken under X100 magnification. Tapping mode on a commercial AFM PS 3000-NS3a was also employed to aid with topography and phase images of the polymer membrane surfaces. SEM and AFM images were performed at Department of Geology, Faculty of Science, University of Malaya.

2.4.2. Mechanical properties

Mechanical measurements were carried out through measuring both tensile strength and elongation percent by using an Instron Universal Testing Machine (Model 4302 Series IX) at Department of Geology, Faculty of Science, University of Malaya.

2.4.3. Thermal stability profile (TGA)

Thermal stability and solid state dehydration changes of membrane samples were carried out using a Mettler-Toledo thermo gravimetric analyzer model TGA/SDTA851e; the measurements were carried out at 500°C at a heating rate of 15°/min, at Department of Chemistry, Faculty of Science, University of Malaya.

2.4.4. Antimicrobial activity of composite membrane

Gram-negative *Pseudomonas* sp. and gram-positive *Staphylococcus* sp. bacterial strains were received from the antibiotic standard used: Amikan (AK) of Microorganisms. The bacteria were grown and maintained in nutrient agar disk diffusion No. 1 (Fluka). Microbial suspensions were prepared in a sterilized physiological solution. Fifty microliter suspensions containing $(4-5) \times 10^5$ cells/mL were diluted in 50 mL of a physiological solution and then were filtered through the membrane at an operating pressure of 200 kPa. After filtration, the membranes Scheme 1 chemical transformations of cellulose modification were incubated on nutrient agar medium for 24 h at 30°C. The bactericidal activity was determined in terms of the growth inhibition, which was calculated by the following equation: Growth inhibition ¼ N1_N2/N1 × 100%, where N1 and N2 are the numbers of viable colonies on control and modified membranes, respectively. An unmodified membrane was used as a control and for comparison.

3. Results and discussion

The description of membranes selected for this study is shown in Table 1. The selection was done according to good water flux with acceptable salt rejection [22].

3.1. Calibration of RO properties of different synthetic composite membranes

RO properties of different types of synthetic composite membranes were calibrated against Film Tech SW30 membrane that was already used in the desalination station in Egypt. This calibration was carried out by comparing the values of both salt rejection and water flux as shown in Table 2, using reverse osmosis laboratory unit at the operation conditions of NaCl solution (EC 15,000 μ mohs), 30 bar applied pressure, flow rate 3 l/min for 6 h as the operation time.

3.2. Scanning electron microscopy

Revealing the microstructure of the various components of the membrane could be regarded as a useful tool when interpreting durability and function values. Accordingly, Fig. 5 exhibits the scanning

Table 1
Multilayer membranes description

Membrane	Added layer	Synthesis technique	Ratio (%)	Thickness μ
PVA/CA	PEG1	Chemically technique	5	70
PVA/CA	PEG2	Chemically technique	10	100
PVA/CA	PEG3	Chemically technique	15	180
PVA/CA	PEG4	Chemically technique	20	220

Table 2
Comparison of reverse osmosis properties of different synthetic membranes with commercial type membrane (Film Tech SW30)

Membrane type	Reverse osmosis properties	
	R_S (%)	$J_{H_2O} \times 10^{-5}$ (gm/cm^2 s)
Film Tech SW30-8040-A (reference)	64	50
CA and PEG	61	2.47
PVA and CA	49.42	6.77
PVA+CA and PEG	6	84.5

electron micrograph cross-section image for PVA-cellulose composite membrane showing ridge and valley structure ∼0.2–0.5 μm with selective layer at ∼500–1,000 Å. The SEM images revealed the presence of cellulose fiber entanglements on the surface of the membranes. There are slight changes in the surface morphology by addition of maleic acid and increasing porosity due to the increase of the number of pores on the surface. This result evidences that the addition of maleic acid to PVA will increase the performance and efficiency of composite membranes.

Mechanical properties are known to be strongly dependent on their morphologies [23]; the homogenous morphology could have influenced the tensile properties of the blends obtained in case of PVA and maleic acid in which the homogenous morphology is accompanied by possessing high tensile and elongation Fig. 6(a–c) illustrates the SEM images of cellulose membrane before soaking with PVA and after PVA and PEG soaking, respectively. Thickening of cellulose fibers, Fig. 7(a), are shown to occur after being coated with CA, Fig. 7(b) after being coated with CA+PVA, Fig. 7(c) after being coated with CA+PVA+PEG and the inner layers become less visible.

Although some diffused features are visible in the uncoated cellulose membranes due to the presence of some open fibrils, but the fibers are apparently smoothened due to coating of the open fibrils with PVA+PEG contrary to PVA membranes, Fig. 6(c)

where smooth and featureless surface without pores are noted. Upon cross-linking by PEG to the CA/PVA material, the morphological feature seems to be more compact and as observed from Fig. 7(c). As acetone was used during membrane casting of the CA, it is expected that the molecules are to be immobilized in a glassy state and no pores formation [26].

3.3. Tapping mode atomic force microscopy

In order to investigate clearly the surface morphology of the composite membranes, AFM was employed; results of which are illustrated in Fig. 7 which shows the images of two- and three-dimensional scans (scale 8 μm) of the CA, PVA, and PVA +CA and PEG membranes [27]. It could be seen from the images, the membrane without PEG showed nearly a unique and consistent characteristic ridge and valley structure [28].

The images demonstrate clearly homogenous morphology and distribution features of CA and PVA, while the PVA+CA and PEG membrane show many irregularities more than that of PVA, with new protuberances and unevenly distributed features. These irregularities may be due to the insufficient coverage of PEG on membrane surface. As a result, the membrane surface was not completely covered by PEG and the uncovered area showed lower position. Therefore, the roughness parameters of the membrane with PEG increased compared to the membrane without its presence [29].

3.4. Thermogravimetric analysis

The TGA was performed on the selected polymers evaluated in this study in order to examine the influence of their structural differences on their degradation behavior [30]. Investigation of TGA of the prepared membranes is presented in Fig. 8 and is interpreted as follow.

According to Fig. 8(a), i.e. PVA thermal degradation, it is seen that the degradation of all synthetic membranes occurs in three steps; (1) the range of first step is from room temperature to 330°C in case of
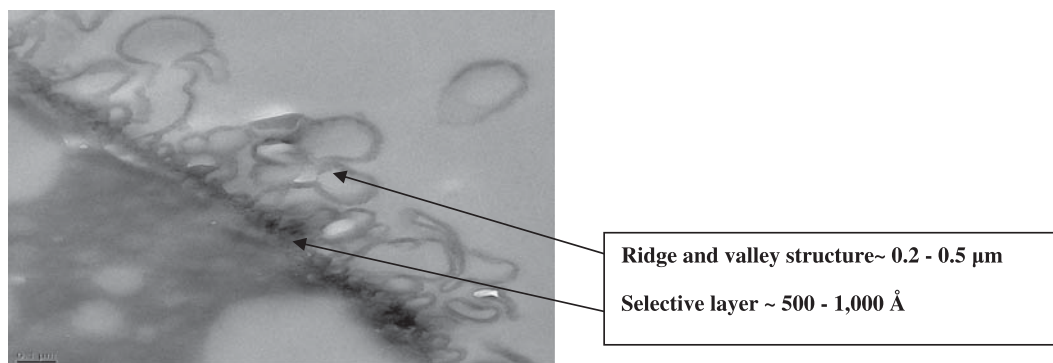
Fig. 5. Cross-section of PVA cellulose composite membrane.
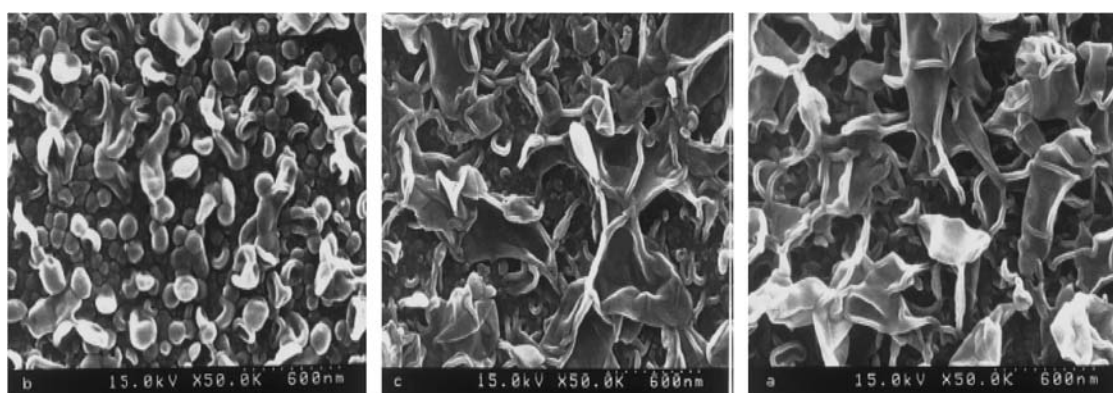
Fig. 6. SEM images of (a) pure cellulose acetate, (b) PVA-cellulose composite membranes, and (c) PVA-CA and PEG composite membrane.
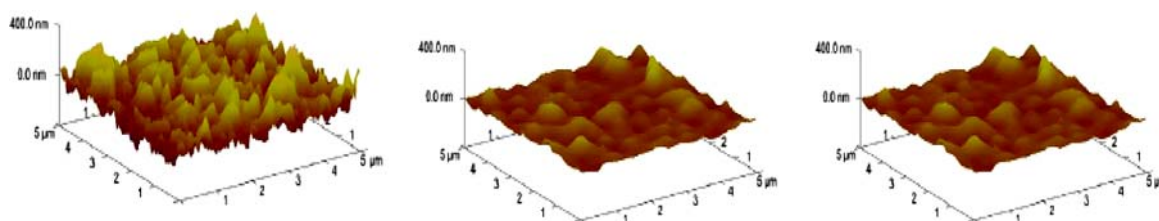
Fig. 7. AFM images showing the 3D surfaces of (a) CA, (b) PVA+CA, and (c) PVA+CA and PEG membrane.

PVA/CA membrane. This step represents the evolution of the volatile matter and/or the evaporation of residual absorbed water. (2) The second step starts from 330 to 380°C which represents the main thermal degradation of the CA chains. (3) The third step takes place over 381°C for PVA/CA membrane which symbolizes the carbonization of the degraded products to ash.

Fig. 8(b), illustrates the degradation of PVA/CA/PEG which takes place also in three steps but is emphasized by more thermal stability than the second composition which may be due to the addition of

Fig. 8. Thermogravimetric profiles of (A) PVA/CA and (B) PVA/CA/PEG membrane.

Table 3
The mechanical properties for some synthetic composite RO membrane

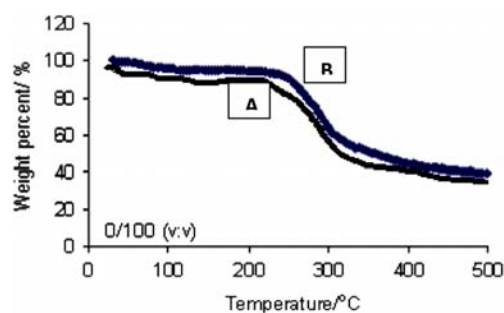| Specimen	Tensile strength yield (MPa)	Yield (%)	Break (MPa)	Elongation break (%)
1	35.98	12.10	14.46	35.14
2	39.91	19.19	59.74	50.34
3	64.22	22.39	21.32	138.10
4	65.34	73.45	76.98	270.87
Mean	38.55	34.63	26.97	85.67
Median	19.67	19.29	19.00	52.53
Minimum	19.40	11.47	7.39	27.29
Maximum	65.30	113.27	76.62	270.17

PEG to the composition, with the thermal degradation from 402°C. Such study proves that the cross-linked PVA/CA membrane by PEG has influenced its thermal stability by nearly 20°C [31,32].

3.5. Mechanical properties

Table 3 shows that the addition of PEG enhanced the resistance of CA and probably reflected the interactions between the free hydroxyl groups of PEG and the chains of CA [33], free COOH groups which enhance the formation of hydrogen bonding leading to cross-linked network structure. This result leads to an increase of tensile strength with a decrease of the elongation percentage.

Effect of CA concentration, PEG additions, solvent effect, and other reaction controlling parameters on the composite membrane quality and performance are reported herein.

3.6. Applications of CA/PEG reverse osmosis membrane in desalination of saline water

We also studied the effect of annealing on the desalination performance of the membranes. Tables 4–6 illustrate the chemical analysis data of pretreated and posttreated seawater sample using PVA, PVA+CA, and PVA+CA and PEG composite membrane after each operating time through desalination process. The selected CA/PEG reverse osmosis membranes were of composition 1:1 CA/PEG copolymer ratio at 100 μ membrane thickness. The selected membrane possesses good mechanical properties (tensile strength = 63.5 MPa and elongation = 49.88%) and suitable R_s and J_{H_2O} for different feed concentrations. Two groundwater samples (brackish, highly saline) and also extremely saline water (sea water) were used. The waste (brine) water was recycled to maintain a constant concentration in the feed tank by adding distilled water and is briefed as follows.

3.6.1. Desalination of highly saline water (sea water)

The feed of seawater (TDS = 13986.07 ppm) of slightly alkaline pH = 7.4 is pumped into a closed vessel in the RO unit, where it is pressurized at 40 bar with a flow rate of 3 l/min against the RO membrane. This pressure value is needed to enable the fresh water to pass through the membrane leaving an amount of rejected salts; some amounts of salts passed through the membrane and remained in the product water. The results show that the total mineralization (water salinity) as well as the ionic composition of the groundwater decrease gradually as a function of desalination operation time. By using the selected membrane, the values of electric conductivity and total dissolved solids of posttreated water became 12,850 μm hos, 7,036 mg/L, 10,750 μm hos, 5,857 mg/L, and 9,050 μm hos, 5,059 mg/L at operation times of 8, 16, and 24 h, respectively, are shown in Table 7.

3.6.2. Desalination of brackish water

The feed of brackish water (TDS = 3,333 ppm) of slightly alkaline pH (7.8) is pumped into a closed vessel in the RO unit, where it is pressurized by 30 bar with a flow rate of 5.1/min against the RO membrane. This pressure is needed to enable the fresh water to pass through the membrane leaving an amount of salts rejected; some amounts of salts passed through the membrane and remained in the produced water. The results show that the total mineralization (water salinity) as well as the ionic composition of the saline water decrease gradually as a function of desalination operation time. By using the selected membrane, the values of electric conductivity and total dissolved solids of posttreated water became 2,800 μm hos, 1,620 mg/L, 2,200 μm hos, 1,301 mg/L, and 1,680 μm hos, 933 mg/L for operation times of 5, 8, 16, and 24 h, respectively, as shown in Table 8.

3.6.3. Desalination of seawater (extremely saline water)

The feed concentration of seawater (TDS = 42,847 mg/L) and alkaline pH = 7.9 is pumped into a closed vessel in the RO unit, where it is pressurized at 50 bar against the PVA/CA/PEG composite membrane. The results show that the total mineralization (water salinity) and the ionic concentration of the groundwater decrease gradually as a function of operation time increase. By using the selected membrane, the values

Table 4
Chemical analysis data of pretreated and posttreated extremely saline water samples using CA and PEG reverse osmosis membrane

Operation time	TDS (mg/L)	Unit	Ca^{++}	Mg^{++}	Na^{+}	K^{+}	Total cations	CO_3^-	HCO_3^-	SO_4^-	Cl^-	Total anions	Hypothetical salts (%)				
													NaCl	$MgCl_2$	$CaCl_2$	$CaSO_4$	$Ca(HCO_3)_2$
Pre-treatment (row water)	13,986.07	mg/L	1,009	589.3	3261	60	242.19	0	244	1970	6975	241.69	59	20	3	16	2
		me/L	50.34	48.46	141.85	1.53		0	3.99	41.02	196.70						
		%	20.79	20.01	58.57	0.63		0	1.65	16.97	81.38						
Produced water after 8 h	7,036.78	mg/L	582	259.3	1630.5	20	121.80	0	134.2	950	3534	121.43	58	18	6	16	2
		me/L	29.04	21.32	70.93	0.51		0	2.19	19.78	99.66						
		%	23.84	17.51	58.23	0.42		0	1.64	16.29	82.07						
Produced water after 16 h	5,856.81	mg/L	388	188.6	1535.5	17	102.10	0	122	520	3162	101.49	66	15	6	11	2
		m/L	19.36	15.51	66.79	0.43		0	1.99	10.83	89.17						
		%	18.96	15.19	65.42	0.43		0	1.47	10.67	87.86						
Produced water after 24 h	5,059.11	mg/L	213.4	153.2	1442	17	86.41	0	91.5	320	2883	88.96	73	15	3	7	2
		me/L	10.65	12.60	62.73	0.43		0	1.49	6.66	81.30						
		%	12.32	14.58	72.60	0.50		0	1.12	7.49	91.39						

Table 5
Chemical analysis data of pretreated and posttreated highly saline water samples using PVA+CA reverse osmosis membrane

Operation time	TDS mg/L	Unit	Ca^{++}	Mg^{++}	Na^{+}	K^{+}	Total cations	CO_3^-	HCO_3^-	SO_4^-	Cl^-	Total anions	Hypothetical salts (%)				
													NaCl	$MgCl_2$	$MgSO_4$	$CaSO_4$	$Ca(HCO_3)_2$
Pre-treatment (raw water)	3,333	mg/L	334.8	180.8	614	5.09	58.41	0	244	900	1176	55.89	46	18	7	22	7
		me/L	16.71	14.87	26.70	0.13		0	3.989	18.73	33.16						
		%	28.6	25.46	45.72	0.22		0	7.14	33.53	59.33						
Produced water after 8 h	1,620	mg/L	167.4	79.1	316.6	1.82	28.67	0	122	370	624	27.29	48	17	6	22	7
		me/L	8.353	6.505	13.77	0.04		0	1.99	7.7	17.59						
		%	29.13	22.68	48.03	0.16		0	7.42	28.22	64.27						
Produced water after 16 h	1,301	mg/L	130.2	56.5	252	1.36	22.14	0	106.8	280	528	22.46	50	15	6	21	8
		me/L	6.497	4.65	10.96	0.034		0	1.74	5.82	14.88						
		%	29.33	21	49.51	0.16		0	7.77	25.39	64.84						
Produced water after 24 h	933	mg/L	93	33.9	209	1.36	16.53	0	76.25	150	408	15.87	55	14	3	20	8
		me/L	4.641	2.79	9.07	0.034		0	1.24	3.123	11.50						
		%	28.07	16.86	54.86	0.21		0	7.85	18.79	69.21						

Table 6
Chemical analysis data of pretreated and posttreated seawater sample using PVA+CA and PEG composite membrane after each operating time through desalination process

Operation time	TDS (mg/L)	unit	Ca^{++}	Mg^{++}	Na$^+$	K$^+$	Total cations	CO$_3^-$	HCO$_3^-$	SO$_4^-$	Cl$^-$	Total anions	NaCl	MgCl$_2$	Mg SO$_4$	CaSO$_4$	Ca(HCO$_3$)$_2$
Pre-treatment (raw water)	42847.12	mg/L	520.8	1672	12,902	380	734.48	0	244	4000	23,250	742.92	77	11	8	3	1
		me/L	25.99	137.53	561.24	9.72		0	3.99	83.28	655.65						
		%	3.54	18.73	76.41	1.32		0	0.54	11.21	88.20						
Produced water after 8 h	24689.96	mg/L	334.8	836.2	7500	240	417.86	0	183	2900	12,788	423.98	80	5	11	3	1
		me/L	16.71	68.77	326.25	6.14		0	2.99	60.38	360.61						
		%	3.99	16.46	78.08	1.47		0	0.71	14.24	85.05						
Produced water after 16 h	21946.01	mg/L	297.6	723.2	6714	210	371.75	0	152.5	2300	11,625	378.20	80	5	11	3	1
		me/L	14.85	59.47	292.06	5.37		0	2.49	47.89	327.83						
		%	3.99	16.00	78.57	1.44		0	0.66	12.66	86.68						
Produced water after 24 h	16721.95	mg/L	223.2	542.4	5104	102	280.38	0	122	1680	9009.4	291.04	80	6	10	3	1
		me/L	11.14	44.61	222.02	2.61		0	1.99	34.98	254.06						
		%	3.97	15.91	79.19	0.93		0	0.69	12.02	87.29						

of electric conductivity and total dissolved solids of posttreated water became 39,200 μmhos, 24,690 mg/L; 34,350 μmhos, 21,946 mg/L; and 27,500 μmhos, 16,722 mg/L at operation times of 8, 16, and 24 h, respectively, and is shown in Table 9.

The salt rejection rate decreased with increasing feed salt concentration but remain unchanged when the ratio of membrane charge density to feed concentration was kept constant. Shielding of membrane charge to a large operating pressure is due to the effect of Donnan exclusion which reduces with increasing feed electrolyte concentrations. This type of retention sequence was observed by several other authors as well and is attributed to the negative charge of the PVA+CA and PEG composite membrane used [34–37] resulting in a low effective charge as depicted in Table 10.

3.7. Antimicrobial activity of the composite membrane

In recent years, self-sterilizing surfaces have attracted growing interest. Products with an added antimicrobial treatment are finding excellent acceptance by the medical community. They include surgical drapes, instrument wraps, and surgical packs that reduce the risk of postoperative infection [38] and tooth fillings [39]. Microbiological evaluations have been carried out on a variety of textile materials [40] and food packaging [41] treated with antimicrobial agents. They have been treated against a broad spectrum of micro-organisms, including odor-causing bacteria as well as bacteria and fungi, which cause rot and mildew. Most such materials are based on compositions that release biocidal molecules or ions. However, the application of polymer biocides has opened new frontiers in the development of nonleaching antibacterial surfaces [42,43]. Recently, attempts have been made to render antimicrobial membrane surfaces by graft copolymerization and interfacial polycondensation of amine-containing polymers, which are potentially antimicrobial agents [44,45].

In this study, composite membrane with antimicrobial properties are well documented [46,47] and was tethered onto the surfaces of cellulose membranes to provide them biocidal activity and thereby lower the membrane biofouling potential. To render the surface of ultra filtration membranes biocidal, cellulose membranes were modified with PVA, a naturally occurring polycationic biocide. Through the use of membranes with different pore sizes, the alteration of the morphological structure of composite layers was achieved. The importance of such structural differences in the antimicrobial activity of the prepared membranes against gram-negative *Escherichia coli* was studied. The antimicrobial efficiency improved with the use of composition

Table 7
Reverse osmosis parameters for the PVA/CA+PEG membrane in desalination of highly saline water sample

Time (h)	R (%)	Salt passage (%)	$J_w \times 10^{-5}$ (gm/cm^2 s)	Salinity of pre-treated water (row water) (mg/l)	Salts (%) of TDS of feed concentration				
					NaCl	MgCl$_2$	CaCl$_2$	CaSO$_4$	Ca(HCO$_3$)$_2$
0	0	100	0	13,986	59	20	3	16	2
				Salinity of post-treated water (mg/L)	Salt rejection (%)				
					NaCl	Mg Cl$_2$	Ca Cl$_2$	Ca SO$_4$	Ca(HCO$_3$)$_2$
8	49.7	50.31	13.88	7036.78	29.82	10.94	−0.02	7.95	0.99
16	58.1	41.88	10.80	5856.81	31.36	13.72	0.49	11.39	1.16
24	63.8	36.17	9.26	5059.11	32.59	14.57	1.91	13.47	1.28

Table 8
Reverse osmosis parameters for the PVA/CA+PEG membrane in desalination of brackish water sample

Time (h)	R_s (%)	Salt passage (%)	$J_w \times 10^{-5}$ (gm/cm^2 s)	Salinity of pre-treated water (row water) (mg/l)	Salts (%) of TDS of feed concentration				
					NaCl	MgCl$_2$	MgSO$_4$	CaSO$_4$	Ca(HCO$_3$)$_2$
0	0	100	0	3,333	46	18	7	22	7
				Salinity of post-treated water (mg/l)	Salt rejection (%)				
					NaCl	MgCl$_2$	MgSO$_4$	CaSO$_4$	Ca(HCO$_3$)$_2$
8	51	49	15.43	1,619.9	22.67	9.74	4.08	11.31	3.60
16	61	39	14.20	1,301.4	26.47	12.14	4.66	13.80	3.88
24	70	28	10.28	932.8	30.60	14.08	6.16	16.40	4.76

Table 9
Revere osmosis parameters for the PVA/CA+PEG in desalination of seawater sample

Time (h)	R (%)	Salt passage (%)	$J_w \times 10^{-5}$ (gm/cm^2 s)	Salinity of pre-treated water (row water) (mg/l)	Salts (%) of TDS in feed concentration				
					NaCl	MgCl$_2$	MgSO$_4$	CaSO$_4$	Ca(HCO$_3$)$_2$
0	0	100	0	42,847	77	11	8	3	1
				Salinity of post-treated water (mg/l)	Salt rejection (%)				
					NaCl	Mg Cl$_2$	Mg SO$_4$	Ca SO$_4$	Ca(HCO$_3$)$_2$
8	42.4	57.62	12.85	24689.96	30.90	8.12	1.66	1.27	0.42
16	48.8	51.22	11.82	21946.02	36.02	8.44	2.36	1.46	0.49
24	60.9	39.03	8.18	16721.95	44.77	8.65	4.09	1.83	0.61

Table 10
Comparison between salt rejection and water flux of brackish, highly saline groundwater, and seawater samples

Parameter	Raw water (mg/l)	Permeate conc. (TDS mg/L)	R_s (%)	$J_w \times 10^{-5}$ (gm/cm^2 s)
Brackish water	3333	933	69.62	10.28
Highly saline water	13,986	5059	63.36	9.26
Sea water	42,847	16,722	59.14	8.18

with higher molecular weights and membranes with smaller pore sizes. This suggested that the surface location of the grafted membrane chains was more preferential for a higher antimicrobial activity of the surface. Membranes modified with PEG showed higher antimicrobial efficiency against gram-positive (*Staphylococcus* sp.) and gram-negative (*Pseudomonas* sp.). Gram-positive bacteria and gram-negative bacteria gave a positive result with the membrane which gave an inhibition zone that indicated that the composite membrane kills these bacteria.

pores of membrane. The importance of such structural differences for antimicrobial activity of the prepared membranes has been studied with the use of gram-negative and gram-positive bacteria. The highest antimicrobial activity of modified membranes is achievable when the degree of membrane modification is close to its maximal value. Antimicrobial efficiency improves with the use of PEG and membranes with smaller pore sizes. It is believed that immobilized biocides must be sufficiently long to traverse and damage the cellular membrane/wall of bacterial cells in contact with the surface. Modification of membranes with

Pseudomonas sp. (gram −ve)   *Staphylococcus sp. (gram +ve)*

4. Conclusions

The PVA/CA/PEG composite multilayer membrane is acceptable for practical uses in desalination of brackish, highly saline, and sea (extremely saline water) water, where the salt rejection (%) was 70, 63, and 59, respectively. In other words, the water salinity of brackish (3,333 mg/L), highly saline groundwater (13,986 mg/L), and seawater (42,847 mg/L) became 933, 5,059, and 16,722 mg/L after desalination time of 24 h for one run of such membrane but these values of produced water salinity can be decreased by increasing the number of the used membranes. Therefore, after treatment of brackish groundwater sample, the obtained produced water has a low value of TDS (933 mg/L), which is accepted by International standards because this salinity is suitable for human consumption of drinking water, Table 6. On the other hand, the water flux decreases with increasing feed concentration during operating time of 24 h, where water flux was 10.32, 9.26, and 8.18 (gm/cm^2 s $\times 10^{-5}$) for brackish, highly saline, and seawater, respectively. The lowering of water flux with the increase of operation time is due to the accumulation of the salts in the

smaller pore sizes occurs entirely on the membrane surface when membranes are modified with PEG. This results in the most expanded layer of bound PEG with the highest activity against *Staphylococcus* and *Pseudomonas*. Consequently, the decrease in the antimicrobial efficiency with the increase in the pore size is more pronounced when membranes are modified with low-molecular weight PEG.

References

[1] M.A. House, D.H. Newsome, Water quality indices for the management of surface water quality, Water Sci. Technol. 21 (1989) 1137–1148.
[2] S.B. Jonnalagadda, G. Mhere, Water quality of the Odzi river in the eastern highlands of Zimbabwe, Water Res. 35 (2001) 2371–2376.

[3] S.M. Liou, S.L. Lo, C.Y. Hu, Application of two-stage fuzzy set theory to river quality evaluation in Taiwan, Water Res. 37 (2003) 1406–1416.

[4] A.J. Melloul, M. Collin, A proposed index for aquifer water quality assessment: the case of Israel's sharon region, J. Environ. Manage. 54 (1998) 131–142.

[5] J.W. Nagel, A water quality index for contact recreation, Water Sci. Technol. 43 (2001) 285–292.

[6] S.G. Nives, Water quality evaluation by index in Dalamatia, Water Res. 33 (1999) 3423–3440.

[7] S.F. Pesce, D.A. Wunderlin, Use of water quality indices to verify the impact of Cordoba city (Argentina) on Suquia river, Water Res. 34 (2000) 2915–2926.

[8] D.G. Smith, A new form of water quality index for rivers and streams, Water Sci. Technol. 21 (1989) 123–127.

[9] G. Muldowney, V. Punzi, A comparison of solute rejection models in reverse osmosis membranes for the system water–sodium chloride–cellulose acetate, Ind. Eng. Chem. Res. 27 (1988) 2341–2345.

[10] B.K. Dutta, S. Harimurti, S. Chakrabarti, D. Vione, Degradation of diethanolamine by Fenton's reagent combined with biological post-treatment, Desalin. Water Treat. 19 (2010) 286–293.

[11] A.R. Khataee, B. Habibi, Photochemical oxidative decolorization of CI basic red 46 by UV/H_2O_2 process: optimization using response surface methodology and kinetic modeling, Desalin. Water Treat. 16 (2010) 243–253.

[12] P. Kumar, T.T. Teng, S. Chand, K.L. Wasewar, Fenton oxidation of carpet dyeing wastewater for removal of COD and color, Desalin. Water Treat. 28 (2011) 260–264.

[13] L.G. Devi, S.G. Kumar, K.M. Reddy, C. Munikrishnappa, Effect of various inorganic anions on the degradation of Congo Red, a di azo dye, by the photo-assisted Fenton process using zero-valent metallic iron as a catalyst, Desalin. Water Treat. 4 (2009) 294–305.

[14] Z. Xiang-hua, Y. Shui-li, W. Beii-fu, Z. Hai-feng, Flux enhancement during ultrafiltration of produced water using turbulence promoter, J. Environ. Sci. 18 (2006) 1077–1081.

[15] T. Mohammadi, A. Esmaeelifar, Wastewater treatment using ultrafiltration at a vegetable oil factory, Desalination 166 (2004) 329–337.

[16] D. Sun, X. Duan, W. Li, D. Zhou, Demulsification of water in-oil emulsion by using porous glass membrane, J. Membr. Sci. 146 (1998) 65–72.

[17] T. Mohammadi, A. Esmaeelifar, Wastewater of a vegetable oil factory by a hybrid ultrafiltration-activated carbon process, J. Membr. Sci. 254 (2005) 129–137.

[18] M. Ebrahimi, D. Willershausen, K.S. Ashaghi, L. Engel, L. Placido, P. Mund, P. Bolduan, P. Czermak, Investigations on the use of different ceramic membranes for efficient oil field produced water treatment, Desalination 250 (2010) 991–996.

[19] C.B. Spricigo, A. Bolzan, R.A.F. Machado, Separation of nutmeg essential oil and dense CO_2 with a cellulose acetate reverse osmosis membrane, J. Membr. Sci. 188 (2001) 173–179.

[20] K. Scott, A.J. Mahmood, R.J. Jachuck, B. Hu, Intensified membrane filtration with corrugated membranes, J. Membr. Sci. 173 (2000) 1–16.

[21] P. Wang, N. Xu, J. Shi, A pilot study of the treatment of waste rolling emulsion using zirconia microfiltration membranes, J. Membr. Sci. 173 (2000) 159–166.

[22] M.C.V. Vela, S. Blanco, Analysis of membrane pore blocking models applied to the ultrafiltration of PEG, Sep. Purif. Technol. 62 (2008) 489–498.

[23] M. Abbasi, A. Salahi, M. Mirfendereski, T. Mohammadi, A. Pak, Dimensional analysis of permeation flux for microfiltration of oily wastewaters using mullite ceramic membranes, Desalination 252 (2010) 113–119.

[24] S.S. Madaeni, The effect of large particles on microfiltration of small particales, J. Porous Mater. 18 (2001) 143–148.

[25] T. Mohammadi, M. Kazemimoghadam, Chemical cleaning of ultrafiltration membrane in the milk industry, Desalination 204 (2007) 213–218.

[26] F.L. Hua, Y.F. Tsang, Y.J. Wang, Performance study of ceramic microfiltration membrane for oily wastewater treatment, Chem. Eng. J. 128 (2007) 169–175.

[27] D. Elzo, I. Huisman, E. Middelink, Charge effects on inorganic membrane performance in a cross-flow microfiltration process, Colloid Surf., A 138 (1998) 145–159.

[28] Y. Zhao, Y. Xing, N. Xu, Effects of inorganic salt on ceramic membrane microfiltration of titanium dioxide suspension, J. Membr. Sci. 254 (2005) 81–88.

[29] A. Salahi, M. Abbasi, T. Mohammadi, Permeate flux decline during UF of oily wastewater: experimental and modeling, Desalination 251 (2010) 153–160.

[30] L. Yan, S. Hong, M.L. Li, Application of the Al_2O_3-PVDF nano composite tubular ultrafiltration (UF) membrane for oily wastewater treatment and its antifouling research, Sep. Purif. Technol. 66 (2009) 347–352.

[31] M. Kuca, D. Szaniawska, Application of microfiltration and ceramic membranes for treatment of salted aqueous effluents from fish processing, Desalination 241 (2009) 227–235.

[32] R. Ghidossi, D. Veyret, J.L. Scotto, Ferry oily wastewater treatment, Sep. Purif. Technol. 64 (2009) 296–303.

[33] M. Tomaszewska, A. Orecki, K. Karakulski, Treatment of bilge water using a combination of ultrafiltration and reverse osmosis, Desalination 185 (2005) 203–212.

[34] Y.S. Li, L. Yan, C. Bao, Treatment of oily wastewater by organic–inorganic composite tubular ultrafiltration (UF) membranes, Desalination 196 (2006) 76–83.

[35] J. Arévalo, G. Garralón, F. Plaza, B. Moreno, J. Pérez, M.A. Gómez, Wastewater reuse after treatment by tertiary ultrafiltration and a membrane bioreactor (MBR): a comparative study, Desalination 243 (2009) 32–41.

[36] A. Salahi, A. Gheshlaghi, T. Mohammadi, S.S. Madaeni, Experimental performance evaluation of polymeric membranes for treatment of an industrial oily wastewater, Desalination 262 (2010) 235–242.

[37] M. Abbasi, M.R. Sebzari, A. Salahi, S. Abbasi, T. Mohammadi, Flux decline and membrane fouling in cross-flow microfiltration of oil-in-water emulsions, Desalin. Water Treat. 28 (2011) 1–7.

[38] Y. Zhao, Y. Tan, F.S. Wong, Formation of dynamic membranes for oily water separation by crossflow filtration, Sep. Purif. Technol. 44 (2005) 212–220.

[39] A. Salahi, T. Mohammadi, Oily wastewater treatment by ultrafiltration using Taguchi experimental design, Water Sci. Technol. 63 (2011) 1476–1484.

[40] A. Salahi, R. Badrnezhad, M. Abbasi, T. Mohammadi, F. Rekabdar, Oily wastewater treatment using a hybrid UF/RO system, Desalin. Water Treat. 28 (2011) 75–82.

[41] M. Abbasi, M.R. Sebzari and T. Mohammadi, Enhancement of oily wastewater treatment by ceramic microfiltration membrans using powder activated carbon, Chem. Eng. Technol. (2011), DOI: 10.1002/ceat.201100108.

[42] M. Kazemimoghadam, A. Pak, T. Mohammadi, Dehydration of water/1-1dimethylhydrazine mixtures by zeolite membranes, Microporous Mesoporous Mater. 56 (2002) 81–88.

[43] T. Gallego-Lizon, E. Edwards, G. Lobiundo, Dehydration of water/t-butanol mixtures by pervaporation: comparative study of commercially available polymeric, microporous silica and zeolite membranes, J. Membr. Sci. 197 (2002) 309–319.

[44] F.-R. Ahmadun, A. Pendashteh, L.C. Abdullah, D.R.A. Biak, S.S. Madaeni, Z.Z. Abidin, Review of technologies for oil and gas produced water treatment, J. Hazard. Mater. 170 (2009) 530–551.

[45] A. Salahi, T. Mohammadi, A. Rahmat pour, F. Rekabdar, Oily wastewater treatment using ultrafiltration, Desalin. Water Treat. 6 (2009) 289–298.

[46] A. Salahi, T. Mohammadi, Experimental investigation of oily wastewater treatment using combined membrane systems, Water Sci. Technol. 62 (2010) 245–255.

[47] J. Kong, K. Li, Oil removal from oil-in-water emulsions using PVDF membranes, Sep. Purif. Technol. 16 (1999) 83–93.